

Surface islands nucleated by a beam of energetic self-ions

C. P. Flynn, W. Swiech, M. Ondrejcek,* and M. Rajappan

Physics Department and Materials Research Laboratory, University of Illinois at Urbana-Champaign, Urbana, Illinois 61801, USA

(Received 3 August 2007; revised manuscript received 21 October 2007; published 10 January 2008)

Many processes that control materials synthesis hinge on a nucleation event that initiates a first order phase transition. Symmetries that constrain nucleation of elementary nanostructures are therefore of general interest. Using low-energy electron microscopy, we observe the flux at which adatom and advacancy islands nucleate when clean Pt(111), in the temperature range 750–1300 K, is bombarded by a beam of Pt⁺ ions of various energies. The results reveal a previously unobserved symmetry between the chemical potentials μ^* required to nucleate the two types of island. Linear response theory is employed to relate μ^* to ion beam flux; the observations confirm that its use is valid above 1000 K. The observed magnitudes of μ^* agree within a factor 3 with predictions made earlier by Pimpinelli and Villain. In addition, the observations show that adatoms and advacancies on Pt(111) form a strongly reacting assembly, with the life cycle of thermal point defects determined mainly by formation and annihilation as pairs, rather than by processes at fixed sinks such as surface step edges.

DOI: 10.1103/PhysRevB.77.045406

PACS number(s): 68.55.A-, 68.37.Nq, 68.37.-d, 68.49.-h

I. INTRODUCTION

Nucleation is the process that initiates a first order transformation from one phase to a second phase.^{1,2} For a system with N space dimensions, the energy of the $N-1$ dimensional interface creates the bottleneck that controls nucleation when a phase of lower chemical potential μ^* is first created at one location in an expanse of a phase with higher μ^* .^{3,4} For the example of a liquid droplet nucleating from its vapor,¹⁻³ it is the surface energy of the drop that inhibits nucleation. Nucleation at a perceptible rate then requires an excess between vapor and liquid (for a clear introduction, see McDonald⁵). The behavior is ubiquitous. Nucleation is of critical importance in chemical transformations, including precipitation of salts from solution;^{1,2,6} in metallurgy where, for example, molten powders of small, pure particles commonly supercool⁷ to about 80% of the melting temperature T_m ; in technology, as in the growth of chromophores from solution;^{8,9} in surface science, where growth or erosion of crystal layers by atomic beams requires nucleation for each fresh layer;¹⁰⁻¹² in the physics of radiation damage, where irradiation-induced interstitial atoms and vacancies precipitate as dislocation loops^{13,14} and in low temperature physics where, for example, nucleation of B phase ³He from the A phase requires the intervention of cosmic rays.¹⁵

The example concerning nucleation in surface processes, given above, reveals a symmetry that other cases lack. Nucleation is required when atoms, *added* to a complete surface layer, cluster together as an “adatom” island that initiates new layer *growth*, as shown in Fig. 1 (left). It is needed equally in sputtering when *missing* atoms condense, as also shown (right) in Fig. 1, to form an “advacancy” island, that nucleates the *erosion* of the surface layer of a crystal. In this paper we explore the symmetry in the surface conditions needed to nucleate adatom and advacancy islands. Specifically, if growth nucleates at a surface chemical potential μ^* , then erosion must nucleate at the potential $-\mu^*$. This symmetry is expected only when the life cycles of the adatoms and advacancies on the surface are dominated by reactions of

mutual annihilation and creation.¹⁶ Its validity depends, in addition, on a macroscopic view of island energy. The symmetry embraces energetic, kinetic, and thermodynamic components. These several factors are explained below in Sec. III.

The present research employs low energy electron microscopy (LEEM)¹⁷ to observe the evolution of surface nanotopography with time, including island nucleation. Surface step edges are imaged, and their time evolution can be recorded at video rates with lateral resolution ~ 10 nm. By way of illustration, Fig. 2(a) is a LEEM image showing a flat “mesa” on Pt(111), a single terrace $\sim 8 \mu\text{m}$ wide, created by ion beam irradiation¹⁸ (see Sec. V). “Pans” created by similar means, but with steps of opposite sign, provide the advacancy equivalent of the adatom mesa. The profiles are shown idealized in Fig. 2(f). Single-terrace areas of these types, isolated from their surroundings by a perimeter of multiple closely spaced steps, provide excellent experimental testing sites for studies of island nucleation. Figures 2(b) and 2(c), respectively, show the mesa of Fig. 2(a) immediately after nucleation of an adatom island by a beam of $3.7 \mu\text{A cm}^{-2}$ of 65 eV Pt⁺ ions, and after its further growth. Figure 2(d) images an advacancy island nucleated on a pan by a 515 eV beam, and Fig. 2(e) shows many scattered advacancy islands nucleated by a process described in Sec. V. The sign of any particular island is generally known from the evolution of local topography and its response to beams of various energies.

When the flux density is raised in small increments until an island nucleates, the value of μ^* required for nucleation can be determined. From the resulting values of μ^* we are

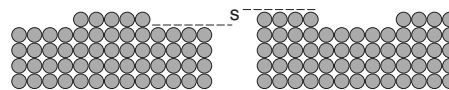


FIG. 1. Sketches showing adatom (left) and advacancy (right) islands on crystal terraces. Circles represent atoms, and the broken line marked s is the terrace surface.

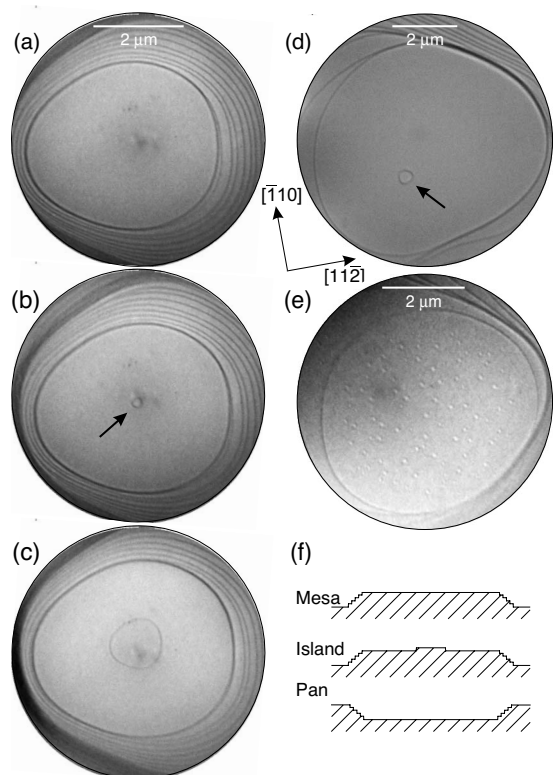


FIG. 2. LEEM images of mesas, pans, and islands on Pt(111). In (a) a mesa comprising a perfect terrace isolated by surrounding downward steps is imaged [see top sketch in (f) for profile]. (b) Same mesa with nucleated adatom island, and (c) after further growth of the island at 1075 K. Nucleation occurred with a flux density $3.7 \mu\text{A}/\text{cm}^2$ of 65 eV ions. The field of view is $5.6 \mu\text{m}$. (d) A pan is shown after nucleation of an advacancy island at 1070 K by $1.1 \mu\text{A}/\text{cm}^2$ of 515 eV ions [see (f) for pan profile]. (e) Multiple vacancy islands nucleated at 845 K by $0.6 \mu\text{A}/\text{cm}^2$ of 515 eV ions; imaged with LEEM electron impact energy $E=17$ eV. (f) Sketches showing mesa, pan, and island profiles.

finally able to address the question of symmetry between adatom and advacancy island nucleation.

The results of the present paper depend in several respects on recent advances described in other publications. As mentioned above, the experiments employ islands created on pans and mesas that are produced by methods detailed elsewhere.¹⁸ Also, quantitative knowledge of the chemical potential μ^* , as created on pans and mesas by ion beams that drive island nucleation, depends both on detailed calibrations of beam damage as a function of energy, and the knowledge that the processes fall in the regime of linear response, all reported in a separate publication.¹⁹ Equally necessary to the present results are earlier measurements of the surface mass diffusion coefficient, over an extended temperature range that includes temperatures of present interest.²⁰ The single chemical potential μ^* , relevant to the driven surface perturbation on the Pt(111) surface at the experimental temperatures, has itself been recognized only recently.¹⁶ Section IV describes how this perturbation of the driven surface depends on the surface mass diffusion coefficient. The quantity μ^* has since been employed in a treatment of the exact linear

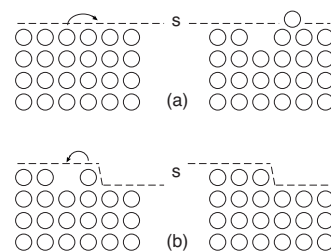


FIG. 3. Point defect processes on terraces. (a) Adatom-advacancy pairs form spontaneously on a perfect terrace, and annihilate by the reverse process. Diffusive hopping can cause adatoms to annihilate or form independently at step edges, with consequent step flow, as illustrated in (b) for the case of advacancy motion. The broken line marked s is the terrace surface.

response of a surface driven by a beam of energetic self-ions.²¹ This treatment provides the basis for the discussion, in Sec. IV, that provides values for the μ^* at which island nucleation is observed to take place. In this way, a quantitative comparison between the present experimental investigations and the predictions of nucleation theory²² is also made possible.

II. SURFACE KINETIC PROCESSES

Diffusion of atoms over metal surfaces proceeds by motion of adatoms and advacancies, with the former believed dominant for many close packed metal surfaces.^{10,11,21,23} The two species are antidefects that form either independently, at step edges, or spontaneously as pairs, from fluctuations of a perfect surface, as in Fig. 3. The defects annihilate either singly or as pairs by the reverse processes. Being thus thermally activated, they occupy a fraction of surface sites (i.e., concentrations) given at equilibrium^{14,21} by

$$\bar{c}_1 = \exp(-g_1/k_B T); \quad \bar{c}_2 = \exp(-g_2/k_B T); \quad (1)$$

here g_1 and g_2 are free energies of formation for adatoms and advacancies. For close packed metal surfaces, the g_i are small enough, and hence the \bar{c}_i sufficiently large, that pair creation and annihilation may dominate the kinetics at temperatures above half the melting temperature T_m .²¹ Then the defect life cycle typically begins with pair creation and ends as pairs annihilate by recombination on an otherwise perfect terrace. Independent processes at steps (see Fig. 3) then largely contribute the difference of the concentrations as the system recovers towards equilibrium after some perturbation such as temperature change.

Using external forces, in our case an ion beam directed onto the terraces, it is possible to drive such an assembly, from equilibrium, to a new steady state in which the changed defect concentrations are c_1 and c_2 . It has been shown that a single chemical potential

$$\mu^* = \frac{k_B T}{2} \left[\frac{\ln \bar{c}_1 \bar{c}_2 \ln(c_1/c_2)}{\ln c_1 c_2} - \ln(\bar{c}_1/\bar{c}_2) \right], \quad (2)$$

then describes the behavior of *both* antidefects.²¹ The relationship between the antidefects may be understood from the

fact that adding an adatom to the assembly has the same effect as removing an advacancy, since both augment the reacting assembly by one atom. Then μ^* is the change of free energy resulting from either of these latter processes. The symmetry on which this paper focuses lies in the values of μ^* required when an ion beam drives the nucleation of adatom and advacancy islands. This criterion is lacking in earlier work that employs separate chemical potentials $\mu_i = k_B T \ln(c_i/\bar{c}_i)$ for the separate defect species, with $i=1$ for adatoms, and $i=2$ for advacancies.¹⁴

In the experiments described below, the external force employed to drive a surface from equilibrium towards nucleation is a beam of self-ions directed along the surface normal. Two competing effects of the ion beam are superposed in the resulting surface perturbation.^{24,25} First, the beam adds atoms to the surface. Second, the energetic collisions create defect pairs and sputter atoms off the surface, both to an extent that increases with impact energy ε . For energies below a “neutral energy” ε_0 the collisions are sufficiently weak and few atoms are sputtered, so the net effect is to create extra adatoms on the surface equal to the beam flux. Above ε_0 , the sputtering exceeds the beam additions and the net result is erosion. In effect, the low-energy beam adds net adatoms that eventually precipitate to grow a new surface layer, while the high energy beam adds net advacancies whose precipitation as islands erodes the existing outer atomic layer. In this way, either growth or erosion can be nucleated by choice¹⁹ of ε . For low ion fluxes, the excess defects created by the perturbation of the beam, after reaction, simply flow to step edges, where their accretion results in growth or erosion by the advance or retreat of the steps. At high fluxes, the nonlinear process of nucleation takes place in addition.

For the case of Pt⁻ ion irradiation of the Pt(111) surface at temperatures above 1000 K, the ion beam intensities required to drive nucleation create only modest perturbations of the surface defect equilibrium. In particular, we show below that the adatom and advacancy populations undergo only small fractional changes. These lie within the range for which the surface, for any particular ion energy, responds linearly to the ion beam intensity. For this regime, the changes of chemical potential caused by an ion beam have recently been predicted explicitly¹⁶ in terms of the surface topography defined by the existing step edges. For large fluxes, still within the regime of otherwise linear response, the nonlinear process of nucleation takes place. These processes are summarized next. The theory allows the value of μ^* required for nucleation to be determined from the ion beam intensity at which new islands spontaneously appear (see Sec. V).

III. SYMMETRY IN NUCLEATION BY AN ION BEAM

There is a rich literature to the theoretical description of homogeneous nucleation.¹⁻⁷ Here we focus on the symmetry of present concern. The early idea that nuclei fluctuate through a critical size to become stable, and thereafter grow without bounds, has survived in current understanding. For the present two-dimensional (2D) case in which islands of

radius a nucleate on a crystal surface, nucleation is controlled by the free energy $2\pi\beta a$ of the step edge that surrounds the island. Here, β is the (1D) free energy per unit length of step.^{10,11,23} In a careful discussion of adatom islands nucleating during sublimation²⁶ (modeled as an ion beam of “negative intensity”), Pimpinelli and Villain²² find nucleation at perceptible rates when μ^* reaches a value μ_{PV}^* given by

$$\mu_{PV}^*/k_B T = 0.2(\beta/k_B T)^2. \quad (3)$$

The experiments described below provide a test of this prediction.

The symmetry of nucleation on which we focus has been proposed¹⁶ in recent research concerning driven surfaces. It has thermodynamic, energetic and kinetic components that are now summarized for the reader’s convenience.

The *thermodynamic* behavior of interest concerns the linear response of surfaces to the driving force of defect creation. If, on a pan or mesa of radius R , adatoms and advacancies are created at rates (per atomic surface site) of K_1 and K_2 , then the chemical potential at radius r on the terrace, in the limit of strongly reacting antidefects, takes the form¹⁶

$$\mu^*(r) = \frac{k_B T(K_2 - K_1)}{4(D_1\bar{c}_1 + D_2\bar{c}_2)} [R^2 - r^2]. \quad (4)$$

As μ^* is largest at $r=0$, nucleation generally occurs near the terrace center where $\mu^* \approx \mu^*(0)$. The important points are that (i) the creation rates K_1 and K_2 , drive $\mu^*(0)$ linearly; and (ii) the value depends only on the *difference* $\Delta K = K_1 - K_2$ of adatom and advacancy rates (rather than on, for example, their separate concentrations). The reason for this dependence may be stated concisely: In the limit of strong reactions, all defects recombine except for the excess, ΔK , which thus comprises the net perturbation driving μ^* in Eq. (4). The linear responses to the adatoms and advacancies created by the uniform beam are spatially identical, and simply superpose in the result of Eq. (4).

Consider next the *energetics* of the nucleation process. In the two parts of Fig. 1, the added free energy of the islands over that of perfect lattice with the same number of occupied sites is, as stated above, $2\pi\beta a$ for *both* adatom and advacancy islands. This is the case because the energy of a curved step does not depend on the sign of its curvature. With A the area per atom, $n = \pi a^2/A$ adatoms must have precipitated for an island this size, so that for an excess defect potential μ^* , the total free energy excess is²² $F(a) = 2\pi\beta a - \pi a^2 \mu^*/A$. For the complementary case in which precipitation of $\pi a^2/A$ advacancies is driven by the reversed potential $-\mu^*$, the *identical* expression is obtained for the free energy increase $F(a)$. (Note that an adatom transferred from μ^* to 0 requires the same free energy change as an advacancy transferred from $-\mu^*$ to 0, since the values of dF/dn are opposite for the two antidefects). Thus within the limits of the macroscopic modeling of the step edge, the energetics of adatom nucleation for μ^* as a function of content n are identical to the nucleation energetics of advacancies for $-\mu^*$. Their common variation of F with a is shown in Fig. 4. The kinetic bottleneck to nucleation occurs where F passes through a maxi-

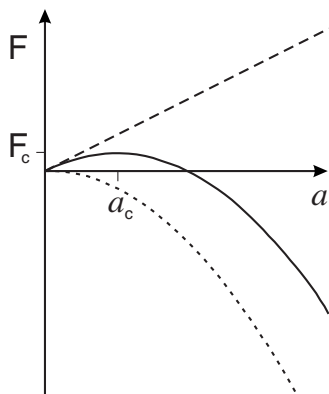


FIG. 4. The free energy F of adatom islands as a function of radius a , for a positive chemical potential μ^* . Broken lines depict the free energy of the perimeter step (positive, linear) and of the precipitated ions (negative, quadratic). Subscripts c mark values for maximum F , above which islands grow freely. The identical $F(a)$ describes the free energy of an advacancy island growing when the chemical potential is $-\mu^*$.

mum F_c at the critical radius a_c . In summary, the present discussion affirms that a_c and F_c are identical for adatom and advacancy nucleation, within this model.

We turn finally to the role of *atomic transport* in the symmetry between adatom and advacancy island nucleation. A key feature is that adatom islands grow by addition of adatoms or, equally, by emission of advacancies; the reversed transport fluxes describe the growth of advacancy islands. From the Nernst-Einstein equation, transport is known to be driven linearly by a gradient of μ^* :

$$J = -(D_s/k_B T) \nabla \mu^*(r), \quad (5)$$

in which $D_s = D_1 \bar{c}_1 + D_2 \bar{c}_2$ is the surface mass diffusion coefficient²¹ for the reacting assembly. Indeed, the same basis in Eq. (5) explains the form of Eq. (4). The important point here is that the flow over the nucleation barrier F_c in Fig. 4 must follow this general form and, as a result, is identical for adatom and advacancy islands, given the equal driving forces $\pm\mu^*$ and the identical nucleation barriers controlling nucleation. With the rate factors and energetic factors thus quantitatively equivalent, it may be concluded that adatom and advacancy islands must nucleate identically for opposite values of μ^* . A verification of this prediction can both confirm the theoretical basis of the discussion¹⁶ and demonstrate that the defect assembly is indeed reaction limited.

IV. EXPERIMENT

Our experiments employed a LEEM built by Tromp,²⁷ equipped with a SNICS II source of negative ions.²⁸ The ion source as purchased from National Electrostatics Corporation provides ion beams with energies up to 20 keV. Low electron impact energies are valuable in LEEM as they improve the amplitude of the backscattering signal employed for imaging. Also, atomic steps are then a fraction of one wavelength high, and are made visible in an image by diffraction contrast. The newly operational LEEM-SNICS II

tandem is described elsewhere.²⁹ It provides beams of selected ions, with energy tunable in the range 0–5 keV, on a sample held near -15 keV (as is common in existing LEEM designs). The maximum ion beam intensity up to $20 \mu\text{A cm}^{-2}$, achieved for Pt^- , is about 0.1 monolayers per second. The base pressure of the LEEM chamber, in the 10^{-9} Pa range, increased only to $\sim 10^{-8}$ Pa at 1000 K with the ion beam operating.

One main focus of this work necessarily related to cleanliness of the Pt(111) crystal surface. An absence of contamination assumes critical importance here because heterogeneous nucleation at impurity centers could possibly short-circuit the homogeneous nucleation process of interest. The single crystal sample used in this research was 9 mm in diameter and 0.9 mm thick, as purchased from the Surface Preparation Laboratory, The Netherlands. It was cut within 0.2° of the (111) plane. In practice, we observed that nucleation on the cleaned (111) terraces of this crystal took place at successive locations randomly dispersed over the central area of a pan or mesa, barely near steps or flaws where impurities might trap. This pattern of behavior is expected of homogeneous nucleation, since $\mu^* \rightarrow 0$ at step edges, which act as sinks for point defects. Furthermore, owing to the high ambient temperatures employed in the experiments, combined with the low step energies at these temperatures,³⁰ the critical nuclei on Pt(111) are quite large (10 – 10^2 atoms), and this also acts to suppress the influence of impurities.

The required surface perfection was achieved³⁰ by cycles of 1 keV Ar^+ ion bombardment, followed by annealing at 1300 K, with occasional treatment in 10^{-6} Pa O_2 , first in an external chamber and later in the LEEM vacuum. These methods are detailed elsewhere.³⁰ The eventual surface exhibited sharp (1×1) LEED spots with no trace of impurities detected by LEED or Auger probe with 1% sensitivity. Surface temperatures were measured to ± 15 K at 750–1300 K by an infrared optical pyrometer with reflectivity set to 0.3, and also by a disappearing filament pyrometer above 1000 K.

Approximately 60 different island nucleation events were investigated in this research using ions of energy $\varepsilon = 65$ eV for adatom events, and $\varepsilon = 515$ eV for advacancy events. Ion beam currents up to $14 \mu\text{A cm}^{-2}$ were employed.

The LEEM creates images using a microchannel plate, phosphorescent screen, and 8-bit video camera. Sequences of video frames were recorded in DVCPRO format and frames digitized as 640×480 pixel arrays having 256 gray levels. Blank image subtraction improved effective channel plate uniformity (the dark center spot in some images is caused by an insensitive central area). Linear contrast adjustment was occasionally employed. Each image of Fig. 2 reports the full screen image.

The steps on rounded surface hillocks have the appearance of contour loops (see Fig. 2) at uniform height intervals of one layer spacing. An adatom beam causes the areas of the loops to expand. It is predicted by theory and observed in experiments¹⁸ that the inner step expands the most, and joins the second step. With continued beam exposure the two expand together to join the third step, etc. If the beam is controlled to prevent new islands from nucleating, this process can create a mesa of any desired height. Conversely, an ada-

tom beam can create a pan from a smooth surface minimum.¹⁸

V. RESULTS AND DISCUSSION

This research builds on earlier work with ion beams that established facts required in the present work. First, from the evolution of step edge profiles during annealing it has been possible to determine $D_s = 4 \times 10^{-3} \exp(-1.47 \text{ eV}/k_B T) \text{ cm}^2 \text{ s}^{-1}$ over a range 10^6 of values. The experiments included all temperatures employed in the present study.²⁰ Second, from observation of step flow, the rates ΔK of excess defect creation caused by beams of various energy and flux density have been determined.¹⁹ Third, the latter results confirm that the surface responds linearly to the particle flux for flux densities J including those employed here to nucleate new islands.¹⁹ Here, these known values of ΔK and D_s are used in Eq. (4) to determine $\mu_c^*(0)$ for any observed J_c and ε of ion beam. Most work was carried out with beams of energy 65 eV, an “adatom beam,” or 515 eV, an “advacancy beam,” as these provide almost equal but opposite ΔK for equal J .¹⁹ In our investigation of beam-induced nucleation, the sample was first cleaned. A suitable mesa or pan for experimental studies was then created, using the ion beam. Studies of nucleation began after the sample was stabilized at the selected test temperature. The objective was to determine at what flux density J , and hence from Eq. (4), at what value μ_c^* , an island first nucleates. The procedure began at low flux. If no island appeared, the flux was increased by a small factor, typically 10%. This process continued until nucleation was observed. The sample was then stabilized at a new temperature; ion beams were used to remove the new island from the active area; the pan or mesa was refurbished,¹⁸ and a new measurement was begun. The end product of the data collection was a table providing the observed J_c and hence μ_c^* for nucleation as a function of temperature T .

This procedure proved satisfactory at high temperatures. It was simplest for adatom islands nucleating on mesas and advacancy islands on pans. In the remaining cases, for example, adatoms on pans, nucleation could still be initiated and observed without difficulty. However, the beam caused steps that form the pan perimeter to flow inward, so that irradiation over too long a period eventually reduced the effective radius R of the pan. Refurbishing the pan then required irradiation with an advacancy beam. Similar behavior occurred in the converse case of advacancy beams on mesas.

Figure 5 shows the measured critical currents J_c , as determined by these procedures, for ion beam energies of 65 eV (adatom beam, solid circles) and 515 eV (advacancy beam open circles). These results are derived from pans and mesas of various sizes, which affects nucleation. While, for this reason, the points are not fully systematic, the general trend is made clearly apparent as the critical current increases rapidly with T above 1000 K. Given the available beam intensities, the behavior could be followed up to about 1300 K, at which temperature the flux density became insufficient to nucleate islands on terraces of the size studied here. An important point, to which we return below, is that the values of

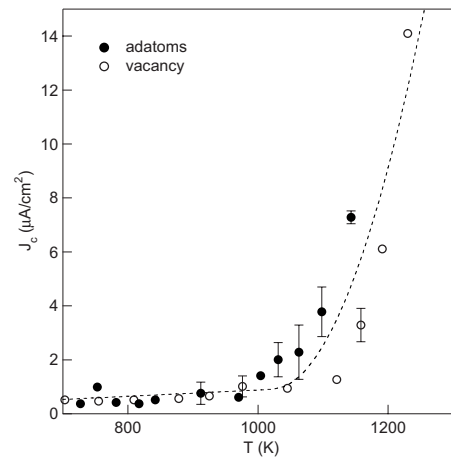


FIG. 5. The ion beam flux density J_c required to nucleate adatom islands (solid circles) and advacancy islands (open circles), shown as a function of temperature. For both species J_c increases rapidly at high T and is constant at low T . The broken line indicates these general trends. The terraces employed lie typically in the range 2–3 μm in radius, and the differences affect the current for nucleation [see Eq. (4)]. In cases with many independent measurements, their scatter is indicated by uncertainty bars.

J_c became insensitive to temperature below about 1000 K.

We turn now to the values of chemical potential at which nucleation was observed. In Fig. 6, the observed values of μ_c^* for Pt^- irradiation of $\text{Pt}(111)$, as derived from the observed J_c in Fig. 5 using Eq. (4), are shown as a function of temperature T by solid circles for adatom islands, and by open circles for advacancy islands. Over the complete temperature range from 730 to 1300 K the adatom and advacancy results track together quite well. This is the most important result of the research. It provides an explicit demonstration that, at all temperatures studied here, adatom and advacancy islands nucleate at equal but opposite values of μ_c^* . This is the new symmetry in nucleation for thermal defect islands, predicted earlier and described above, now confirmed by experiment. As the symmetry is expected only when a system has antidefects with reaction-limited lifetimes, Fig. 6 further confirms that $\text{Pt}(111)$ is reaction-limited above 800 K.

The procedure failed when applied to samples at too high temperature (as detailed above) or too low T . At low T , slow kinetics increased the time required for nucleation, and furthermore, slow diffusion reduced the flux required for a desired μ_c^* . Islands then required greatly lengthened beam exposure to reach a size detectable by LEEM. Delays of minutes, employed in the experiments, were evidently too short for an island to nucleate and grow to visible size. Subsequent flux increases in our experimental procedure then substantially exceeded the critical value actually needed for nucleation. As a result the terrace was driven too strongly by the ion beam, and islands nucleated at many locations. An example displaying this consequence is given in Fig. 2(e).

Lacking alternatives, more than one island on a terrace is taken in what follows as an indication that a quantitative determination of μ_c^* was not achieved.

Three features of Fig. 6 now warrant comment. First, it is

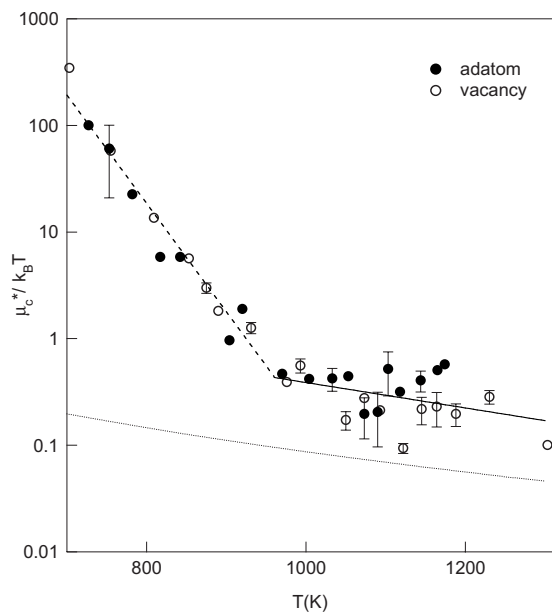


FIG. 6. Chemical potential $\mu_c^*/k_B T$ required for island nucleation, as determined from J_c for Pt⁻ on Pt(111), shown as a function of T for adatom islands (solid circles) and advacancy islands (open circles, with sign of μ^* reversed). The solid line is a least squares fit to all points above 1000 K, and the broken line below 1000 K. The adatom and advacancy results scatter about a common trend throughout, and so verify the symmetry in nucleation on which this work is focused. Below 1000 K, multiple islands nucleate [see, e.g., Fig. 2(e)], and for this reason the points do not identify the correct $\mu_c^*/k_B T$. Above 1000 K, $\mu_c^*/k_B T \ll 1$ so linear response theory is valid. For comparison with the measured values above 1000 K, the dotted line shows $\mu_{PV}^*/k_B T$ as predicted from first principles using the step free energy by Pimpinelli and Villain (Ref. 22).

important that data points *below* about 1000 K, that scatter about the broken straight line, were nearly all cases where multiple (often very many) islands nucleated, as in Fig. 2(e). These are low temperatures cases where the kinetics are slow and the system consequently overdriven. The values of μ^* obtained are thus too large, and to an extent that becomes more severe at lower T . While the deduced μ^* below 1000 K no longer track nucleation of *single* events, the fact that adatom and advacancy islands nevertheless follow a common trend provides a remarkable illustration of the range over which the nucleation properties of the two antidefects are linked. Evidently the symmetry in nucleation behavior occurs more widely than in μ_c alone.

For the data in Fig. 6 *above* about 1000 K, that correspond to single nucleation events, the least square fit shows adatom and advacancy data scattering equally about the mean line. This affords the best indicator of $\mu_c(T)$ for Pt(111). The dotted line a factor ~ 3 below the data shows

the predicted μ_{PV}^* of Pimpinelli and Villain²² [Eq. (3)], taking the measured $\beta = (260 - 0.04 T)$ meV/nm from step fluctuation spectroscopy³⁰ for this range of T . Given the uncertainties of nucleation theory, the comparison appears acceptable.

A third and final matter for concern is the validity of a linear response description of the perturbation caused by the ion beam, as employed here in the analysis of results. Figure 6 shows that $\mu_c^* \leq 0.3 k_B T$, for $T > 1000$ K, where the data provide a valid determination of μ_c^* . The perturbation is thus determined to be a small fraction of $k_B T$. In this important regime, linear response theory therefore remains appropriate, and our demonstration of symmetry between nucleation of adatom and advacancy islands is valid. Below 1000 K, the inferred μ^* reaches values a factor 10^3 larger, which greatly exceed the regime in which the response remains linear. We therefore conclude that our measurements do *not* correctly determine the critical value of μ^* for island nucleation below 1000 K.

VI. SUMMARY

Using LEEM to observe island nucleation, on pans and mesas synthesized on the clean Pt(111) surface, we have employed a beam of Pt⁻ ions to determine the critical chemical potentials μ^* required for the nucleation of adatom and advacancy islands. A recent theory of linear response to the beam-induced surface perturbation is adapted to determine the chemical potential on the irradiated terrace before nucleation. The interpretation makes use of values for the surface mass diffusion coefficient, and a calibration of defect production caused by the ion beam, both available from earlier research. The measurements reported here demonstrate that linear response theory is indeed valid above 1000 K. Advacancy and adatom islands are observed to nucleate at equal but opposite values of μ^* that track together over the temperature range above 1000 K. This newly observed symmetry is a behavior predicted for surfaces on which the life cycle of thermal defects is dominated by pair formation and annihilation reactions, rather than processes at fixed sinks such as step edges. The likelihood that the Pt(111) surface was reaction-limited had been suggested earlier. The absolute values of μ^* at which nucleation takes place are found to agree within a factor 3 with predictions in terms of step free energy β derived from a treatment of nucleation on surfaces.²²

ACKNOWLEDGMENTS

This research was supported in part by DOE under Grant No. DEFG02-02ER46011. The LEEM was maintained in the Center for Microanalysis of Materials in the Materials Research Laboratory, supported by DOE Grant No. DEFG02-91-ER45439.

- *Corresponding author. Fax: +1 217 244 2278. ondrejce@uiuc.edu
- ¹D. Kashchiev, *Nucleation: Basic Theory with Applications* (Butterworth-Heinemann, Oxford, 2000).
- ²F. F. Abraham, *Homogeneous Nucleation Theory* (Academic, New York, 1974).
- ³D. Becker and W. Döring, *Ann. Phys.* **24**, 719 (1935).
- ⁴D. Turnbull and J. C. Fisher, *J. Chem. Phys.* **17**, 71 (1949).
- ⁵J. E. McDonald, *Am. J. Phys.* **31**, 31 (1963).
- ⁶J. W. Mullin, *Crystallization* (Butterworths-Heinemann, Oxford, 2001).
- ⁷D. Turnbull, *Solid State Physics*, edited by F. Seitz and D. Turnbull (Academic Press, New York, 1956), vol. 3, p. 225.
- ⁸L. Brus, *J. Phys. Chem. Solids* **59**, 459 (1998).
- ⁹C. B. Murray, D. J. Norris, and M. G. Bawendi, *J. Am. Chem. Soc.* **115**, 8706 (1993).
- ¹⁰T. Michely and J. Krug, *Islands, Mounds and Atoms* (Springer, Berlin, 2004).
- ¹¹J. W. Evans, P. A. Thiel, and M. C. Bartelt, *Surf. Sci. Rep.* **61**, 1 (2006).
- ¹²B. Mutaftschiev, *The Atomistic Nature of Crystal Growth* (Springer, Berlin, 2001).
- ¹³M. W. Thompson, *Defects and Radiation Damage in Metals* (Cambridge University Press, London, 1969).
- ¹⁴C. P. Flynn, *Point Defects and Diffusion* (Oxford University Press, London, 1972).
- ¹⁵A. J. Leggett, *Phys. Rev. Lett.* **53**, 1096 (1984).
- ¹⁶C. P. Flynn, *Phys. Rev. B* **75**, 134106 (2007).
- ¹⁷E. Bauer, *Rep. Prog. Phys.* **57**, 895 (1994).
- ¹⁸M. Ondrejcek, W. Swiech, M. Rajappan, and C. P. Flynn (unpublished).
- ¹⁹M. Rajappan, W. Swiech, M. Ondrejcek, and C. P. Flynn, *Philos. Mag.* **87**, 4501 (2007).
- ²⁰M. Rajappan, W. Swiech, M. Ondrejcek, and C. P. Flynn, *J. Phys.: Condens. Matter* **19**, 226006 (2007).
- ²¹C. P. Flynn, *Phys. Rev. B* **71**, 085422 (2005).
- ²²A. Pimpinelli and F. Villain, *Physica A* **204**, 521 (1994).
- ²³H-C. Jeong and E. D. Williams, *Surf. Sci. Rep.* **34**, 171 (1999).
- ²⁴R. S. Averback and T. D. de la Rubia, *Solid State Physics*, edited by H. Ehrenreich and F. Spaepen (Academic Press, New York, 1998) Vol. 51, p. 281.
- ²⁵H. Gnaser, *Low-Energy Ion Irradiation of Solid Surfaces* (Springer, Berlin, 1999).
- ²⁶J. J. Metois and D. E. Wolf, *Surf. Sci.* **298**, 71 (1993).
- ²⁷R. M. Tromp and M. C. Reuter, *Ultramicroscopy* **36**, 99 (1991).
- ²⁸R. D. Rathmell, *Rev. Sci. Instrum.* **57**, 727 (1986).
- ²⁹W. Swiech, M. Rajappan, M. Ondrejcek, E. Sammann, S. Burdin, I. Petrov, and C. P. Flynn, *Ultramicroscopy* (to be published).
- ³⁰M. Ondrejcek, W. Swiech, M. Rajappan, and C. P. Flynn, *Phys. Rev. B* **72**, 085422 (2005).